

International Atomic Energy Agency

---

**INDC**

**INTERNATIONAL NUCLEAR DATA COMMITTEE**

---

DOUBLE DIFFERENTIAL CROSS-SECTIONS  
FOR THE (p,n) REACTIONS OF 13.1 MeV PROTONS  
WITH Mo-94,95,96,97,98,100

T. Bröer, E. Mordhorst, S. Stamer, M. Trabant and W. Scobel  
I. Institut für Experimentalphysik  
Bereich Teilchenphysik  
Universität Hamburg  
D-2000 Hamburg 50, Fed. Rep. Germany

NDS LIBRARY COPY

April 1989

---

IAEA NUCLEAR DATA SECTION, WAGRAMERSTRASSE 5, A-1400 VIENNA

DOUBLE DIFFERENTIAL CROSS-SECTIONS  
FOR THE (p,n) REACTIONS OF 13.1 MeV PROTONS  
WITH Mo-94,95,96,97,98,100

T. Bröer, E. Mordhorst, S. Stamer, M. Trabandt and W. Scobel  
I. Institut für Experimentalphysik  
Bereich Teilchenphysik  
Universität Hamburg  
D-2000 Hamburg 50, Fed. Rep. Germany

April 1989

Reproduced by the IAEA in Austria  
April 1989

89-01351

DOUBLE DIFFERENTIAL CROSS-SECTIONS  
FOR THE (p,n) REACTIONS OF 13.1 MeV PROTONS  
WITH Mo-94,95,96,97,98,100

T. Bröer, E. Mordhorst, S. Stamer, M. Trabandt and W. Scobel  
I. Institut für Experimentalphysik  
Bereich Teilchenphysik  
Universität Hamburg

Abstract

Cross sections for the inclusive production of neutrons of  $13.13 \pm 0.15$  MeV protons with all stable Molybdenum isotopes (with the exception of  $^{92}\text{Mo}$ ) have been measured with time-of-flight techniques for 22 angles ranging from  $3^\circ$  to  $177^\circ$ .

1. Introduction

The data presented in this report have been taken as a contribution to the Coordinated Research Program of the IAEA on "Measurement and Analysis of Double-Differential Neutron Emission Spectra in (p,n) and ( $\alpha$ ,n) Reactions". The main objectives of this CRP are:

- (i) to extract systematic information about nuclear level densities as function of excitation energy by analyzing the neutron emission spectra from (p,n) and ( $\alpha$ ,n) reactions on properly selected targets and bombarding energy range, and
- (ii) to parameterize this information into appropriate phenomenological models to enable reliable extrapolation for general use of level density information in basic and applied nuclear physics related problems.

Note

Data in the form of listings can be received from the Nuclear Data Section of the IAEA upon request.

The participants from the University of Hamburg have taken over the task to study the inclusive neutron production from proton induced reactions on Molybdenum isotopes with the time-of-flight facility at the Hamburg Isochronous Cyclotron.

In a first series of measurements we have determined the double differential cross sections for 25.6 MeV protons on all stable isotopes, i.e.  $^{92,94,95,96,97,98,100}\text{Mo}$ . The experiment and its results has been discussed with emphasis on the experimental set up and the systematic and/or statistical uncertainties pertinent to that work in [1]. An interpretation of the results in terms of preequilibrium reaction mechanism has been published, too [2].

In a second series of measurements we have determined the double differential (p,xn) cross sections for  $E_p = 13.1$  MeV. The target  $^{92}\text{Mo}$  has been excluded because of its highly negative Q-value, cf. Table II. The experimental set up is essentially the same as that one described in [1]; in order to make this paper selfcontained, we repeat it here and all the modifications necessary in the conduct of the 13.1 MeV measurements.

## 2. Apparatus and Measurements

### 2.1. Experimental set up

The experiment has been performed with the  $13.1 \pm 0.15$  MeV proton beam of the Hamburg Isochronous Cyclotron. The energy spread includes the effect of the target thickness. The 13.81 MHz repetition rate (cyclotron RF) was scaled down with an external deflection system [3] by a factor of 12 to allow for neutron time-of-flight (TOF) spectroscopy with flight paths of at most 8

m and neutron energies between 1 MeV and 13 MeV without ambiguities due to overlapping bursts.

The geometry of the neutron TOF area is shown in Fig. 1. The set up consists of 8 detectors and is designed for low background and large angular range performance [4]. For this purpose the proton beam is bent with two dipole magnets by  $2 \times 17^\circ$  out of the  $0^\circ$  direction and then dumped into a heavily shielded (water, paraffine, lead) Faraday Cup. The yokes of the magnets are of C type with a gap width of 10 cm. The reaction chamber inserted into this gap has a shape corresponding to a  $34^\circ$  segment of a circle. It has three remotely controlled target positions in front of, between and behind the two magnets. The integrated Faraday Cup current was recorded for absolute cross section determination.

Reaction neutrons from the target position in operation enter flight paths of  $(7.5 \pm 0.5)$  m length through a thin exit window (0.13 mm Kapton foil) towards the neutron detectors. The detectors consist of cylindrical  $4''\phi \times 2''$  cells filled with liquid scintillator NE213 and coupled to photomultipliers VALVO XP2-041. They are viewing the targets through collimator tubes traversing a water shielding of more than 1 m thickness. Conical polyethylene throats at the front ends of the collimator tubes supplement the efficient shielding against time correlated and stray neutrons. The collimator tubes can be aligned towards any of the three optional target positions such that the set up covers an interval of reaction angles  $\theta$  ranging from  $3^\circ$  to  $177^\circ$  with 24 fixed positions and increments of  $6.5^\circ$  for small and large, and  $10.5^\circ$  for intermediate angles, respectively.

The targets were self-supporting, isotopically enriched metallic foils of 12 mm effective diameter and nominal thicknesses

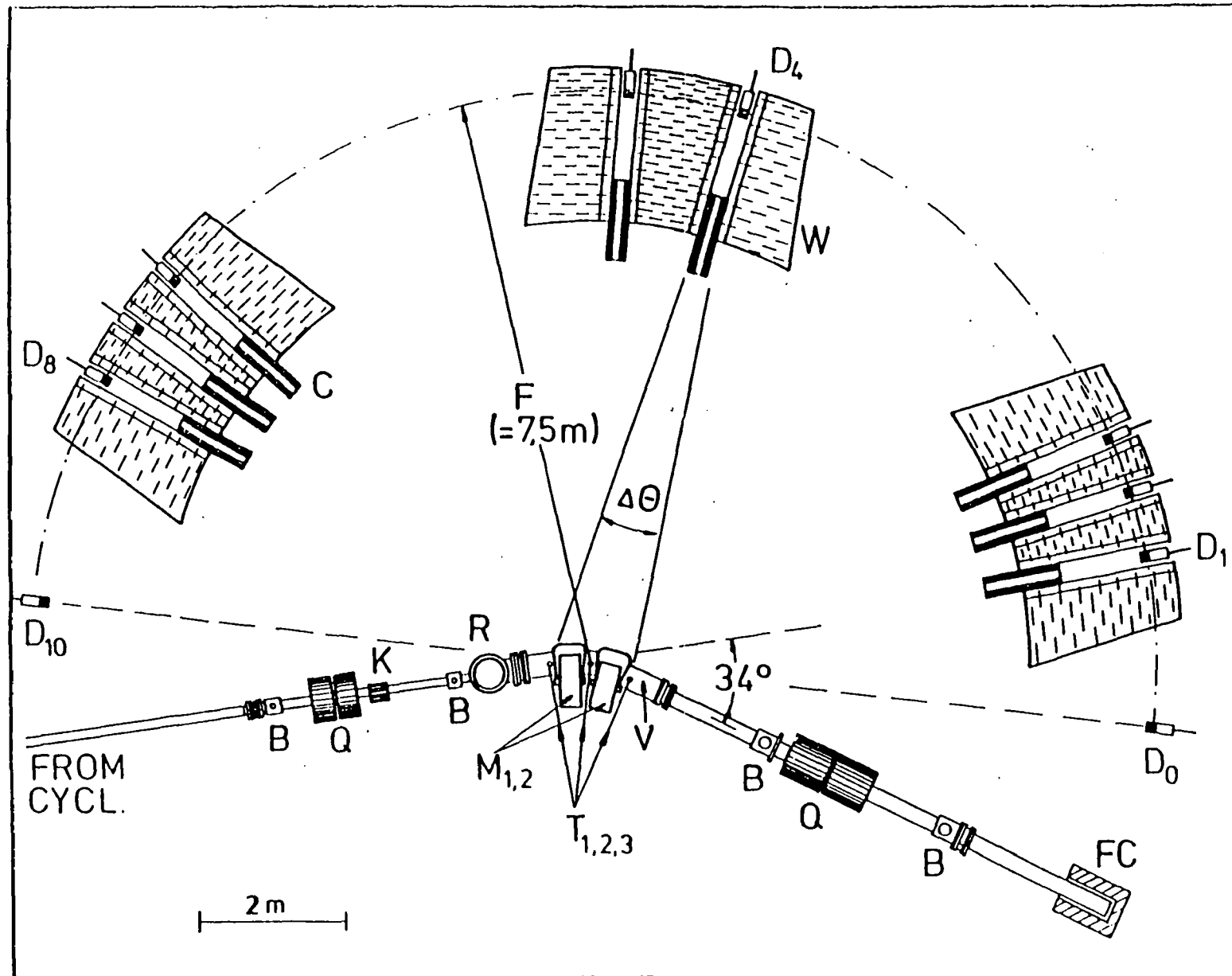


Fig. 1: Layout of the neutron TOF facility (from [4]).

ranging from 3.0 to 4.9 mm/cm<sup>2</sup> (see Table I). Their thicknesses were determined by weighting. The effective thickness in the region of the beam spot of about 4 mm diameter was controlled with the energy loss [5] of <sup>241</sup>Am  $\alpha$ -particles; these values agreed within 5% with those of Table I (exception: <sup>94</sup>Mo, + 12%).

Table I: Target foils and isotopic composition

Target	thickness mg/cm <sup>2</sup>	isotopic constituents (%)						
		92	94	95	96	97	98	100
<sup>94</sup> Mo	2.64	0.87	94.60	2.50	0.98	0.32	0.55	0.18
<sup>95</sup> Mo	4.18	0.14	0.32	97.43	1.38	0.25	0.38	0.09
<sup>96</sup> Mo	4.31	0.13	0.16	0.52	97.67	0.79	0.62	0.11
<sup>97</sup> Mo	4.65	0.22	0.24	0.59	1.34	94.25	3.07	0.30
<sup>98</sup> Mo	4.16	0.10	0.07	0.16	0.23	0.33	98.78	0.33
<sup>100</sup> Mo	4.15	0.12	0.16	0.27	0.38	0.28	0.84	97.95

The electronics of a single neutron TOF detector were conventional. The block diagram of the combined electronics of all 8 detectors is shown in Fig. 2. A linear bias was set individually for each detector at a pulse height corresponding to a proton energy  $E_{\text{thr}} \approx 1.0$  MeV. The exact positions were determined [4] with the Compton edges of sources (<sup>22</sup>Na, <sup>60</sup>Co, <sup>137</sup>Cs, <sup>207</sup>Pb). The photomultiplier signals were stabilized [6] with respect to a stabilized LED. The radiation was effectively suppressed by pulse shape discrimination [7].

The TOF stop signal was derived from the cyclotron radio frequency. The TOF data for neutrons as well as for  $\alpha$  particles were routed via 8 ADC's into an ND4420 multichannel analyzer. The overall time resolution obtained was  $\leq 2.5$  ns (FWHM) corresponding to a neutron energy resolution of up to 100 keV (270 keV) for  $E_n = 5$  MeV (10 MeV).

COMPLETE ELECTRONIC  
CIRCUIT OF THE  
NEUTRON TOF FACILITY

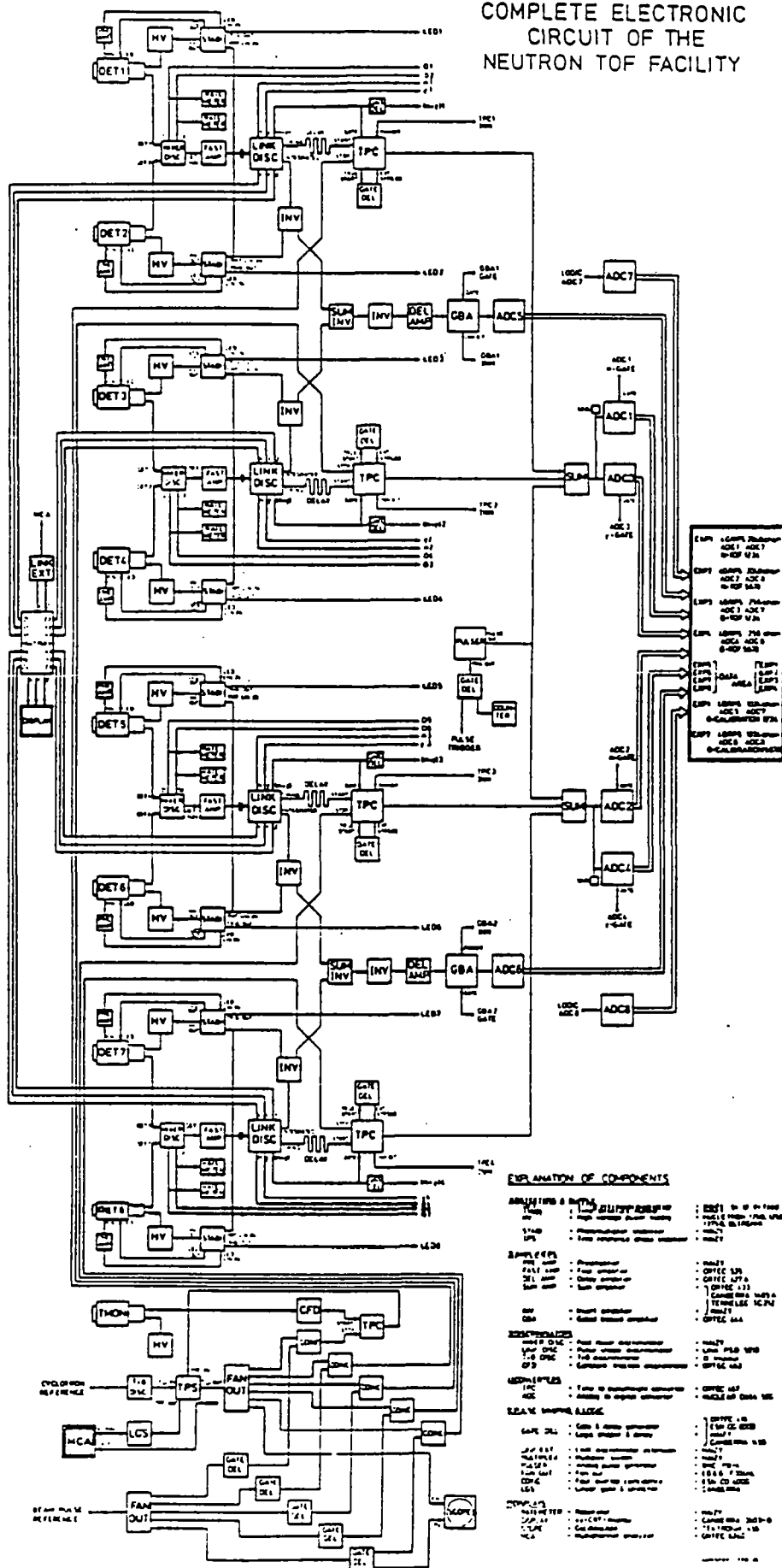


Fig. 2: Electronics diagram.

## 2.2. Measurements and data reduction

The measurements were performed with proton beam intensities of typically 80 nA. For each target and target position a total charge  $Q_{FC}$  of about 1.5 mC was accumulated in the Faraday Cup. Each run was followed by a shorter ( $Q_{FC} \approx 0.5$  mC) background run with shadow bars being placed in the flight paths about midway between target and detectors. The shadow bars are truncated polyethylene cones of 80 cm length (corresponding to 7 attenuation lengths  $\lambda$  for 15 MeV neutrons). However, for the extreme reaction angles  $3^\circ$  and  $177^\circ$ , respectively, carefully aligned shadow bars made out of copper (length: 50 cm, attenuation length for  $E_n = 15$  MeV  $\approx 10 \lambda$ ), that were designed for mounting close to the target, were used instead to account for the worse background conditions due to the upstream beam line and the Faraday Cup, respectively.

The background subtraction represented at most a 10% correction of the integral yield in the physical region  $E_{thr} \leq E_n \leq E_{n,max}$  and was substantial ( $\leq 20\%$ ) only for the extreme angles and the high neutron energies. The energy scale is deduced from the position of the target  $\gamma$  peak and the time calibration of the system. In any case, the background spectra do not exhibit individual structures nor do they reflect the structures in the corresponding target in runs and therefore cannot be responsible for structures in the spectra, which remain after background subtraction. Further experimental details have been reported elsewhere [4,8].

After background subtraction, the TOF spectra were converted with relativistic kinematics into center-of-mass energy spectra of bin size  $\Delta E_n = 100$  keV with the detector efficiencies as described in [9] and under the assumption of single nucleon emission. The Q-values and additional reaction data are listed in

Table II: Reaction data. Maximum kinetic energies (in MeV)  $E_{n,max}$  of the neutrons refer to the c.m.s.

Reaction	$I_{\text{Target}}$	$Q(p,n_0)$	$Q(p,n_1)$	$E_{n,max}$
$^{92}\text{Mo}(p,n)^{92}\text{Tc}$	0 <sup>+</sup>	-8.65	-8.86	4.13
$^{94}\text{Mo}(p,n)^{94}\text{Tc}$	0 <sup>+</sup>	-5.04	-5.12	7.87
$^{95}\text{Mo}(p,n)^{95}\text{Tc}$	5/2 <sup>+</sup>	-2.48	-2.52	10.40
$^{96}\text{Mo}(p,n)^{96}\text{Tc}$	0 <sup>+</sup>	-3.76	-3.79	9.14
$^{97}\text{Mo}(p,n)^{97}\text{Tc}$	5/2 <sup>+</sup>	-1.10	-1.20	11.77
$^{98}\text{Mo}(p,n)^{98}\text{Tc}$	0 <sup>+</sup>	-2.46	-2.48	10.43
$^{100}\text{Mo}(p,n)^{100}\text{Tc}$	0 <sup>+</sup>	-0.95	-1.12	11.93

Table II. The shifts  $E_n$  for neutrons actually resulting from second or third chance emission are at most equal to the recoil correction for the highest possible nucleon energy of  $\approx 10$  MeV (secondary emission), i.e.  $|\pm E_n| \leq 40$  keV. The rare events of neutrons following  $\alpha$  particle emission are neglected.

Having determined the sets of 22 energy spectra for all 6 Molybdenum targets with known isotopic composition (Table I), one can calculate for each bin the double differential cross sections for isotopically pure material from a system of 6 linear equations. All cross sections presented furtheron are unfolded this way.

For one target ( $^{96}\text{Mo}$ ), the measurements under  $\theta_{lab} = 95^\circ$  and  $147^\circ$  failed. Therefore no data are given for any target under these two angles (indicated by values 0.0 in the tables). However, the data for all targets but  $^{96}\text{Mo}$  are available upon request for these angles, too, but without correction for isotopic impurities.

Angle integrated neutron energy spectra were calculated as

$$\frac{d\sigma}{dE_n} = \sum_{v=1}^{22} \frac{d^2\sigma}{dE_n d\Omega}(\theta_v, E_n) \cdot \omega(\theta_v) \quad (1)$$

with the solid angle weighting for  $2 \leq v \leq 21$ :

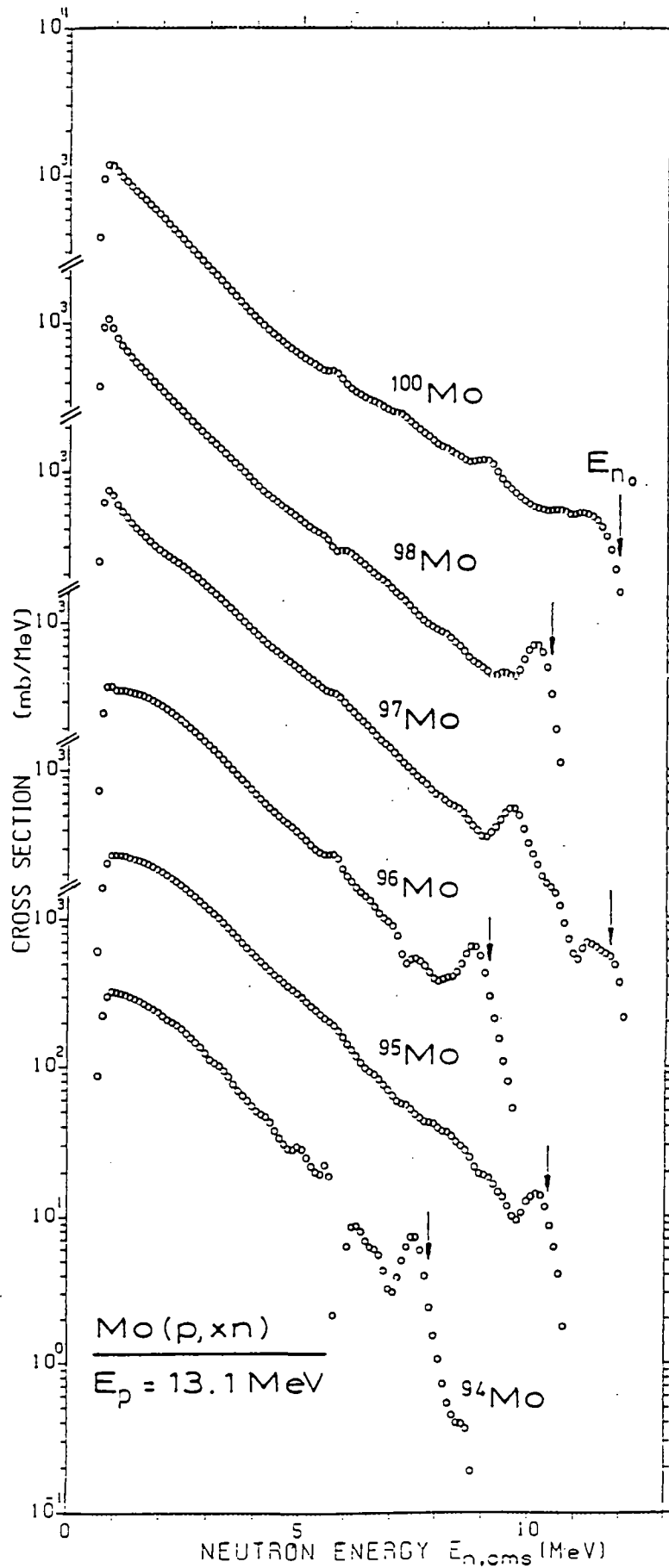


Fig. 3: Angle integrated spectra.

$$\omega(\theta_\nu) = 2\pi \cdot \left[ \cos \frac{\theta_\nu + \theta_{\nu-1}}{2} - \cos \frac{\theta_{\nu+1} - \theta_\nu}{2} \right] \quad (2)$$

and for  $\nu = 1$  or  $22$ :

$$\omega(\theta_\nu) = 2\pi \cdot \left[ 1 - \cos \frac{\theta_\nu + \theta_{\nu'}}{2} \right] \quad (3)$$

where  $\nu' = 21$  (or  $2$ ) for  $\nu = 22$  (or  $1$ ).

The resulting set of angle integrated neutron energy spectra is shown in Fig. 3.

### 2.3. Uncertainty estimates and explanation of tables

The main uncertainty sources and their estimates are:

(1) Neutron detector efficiency	5%
(2) Effective target thickness (due to inhomogeneities and uncertainties of the range-energy tables)	5%
(3) Inconsistencies in the background treatment	5%
(4) Statistical uncertainties (< 1% for $E_n \leq 6$ MeV; < 10% for $E_n \leq 13$ MeV; < 10% for $E_n \leq 20$ MeV)	< 10%
(5) Incomplete beam current integration	3%

The estimated relative uncertainties between neutron spectra obtained in different runs are due to (2)-(5) and should not exceed 10% for all angles and all but the highest neutron energies. Absolute uncertainties are slightly higher due to contribution (1). Therefore we claim absolute uncertainties  $\leq 12\%$  for most of the double differential and all angle integrated cross sections.

The uncertainties given in the tables in the columns labelled PE are given in absolute units and include only the statistical contributions (including background subtraction).

## References

- [1] E. Mordhorst, M. Trabandt, F. Binasch, A. Kaminsky, H. Krause, R. Langkau, W. Scobel and M. Strecker  
Report INDC(GER)-31/GX and Internal Report HH86-10
  
- [2] E. Mordhorst, M. Trabandt, A. Kaminsky, H. Krause, W. Scobel, R. Bonetti and F. Crespi  
Phys. Rev. C34(1986)103
  
- [3] H. Krause, R. Langkau and N. Schirm  
Nucl. Instr. Meth. 134(1976)15
  
- [4] Y. Holler, A. Kaminsky, B. Scharlemann, H. Krause, R. Langkau, W. Peters, G. Poppe, N. Schirm, W. Scobel and R. Wien  
Nucl. Instr. Meth. A235(1985)123
  
- [5] J.F. Ziegler: Helium Stopping Powers and Ranges in All Elemental Matter (Pergamon Press, 1977)
  
- [6] Y. Holler, J. Koch and A. Naini  
Nucl. Instr. Meth. 204(1983)485
  
- [7] J.M. Adams and G. White  
Nucl. Instr. Meth. 156(1978)459
  
- [8] Y. Holler, A. Kaminsky, R. Langkau, W. Scobel, M. Trabandt and R. Bonetti  
Nucl. Phys. A442(1985)79
  
- [9] G. Dietze and H. Klein  
Report PTB-ND-22 (Braunschweig, 1982)